The Impact of Glenoid Labrum Thickness and Modulus on Labrum and Glenohumeral Capsule Function

Nicholas J. Drury
Department of Bioengineering,
University of Pittsburgh,
Pittsburgh, PA 15219
e-mail: drury.nick@gmail.com

Benjamin J. Ellis
e-mail: u0241427@utah.edu

Jeffrey A. Weiss
e-mail: jeff.weiss@utah.edu

Department of Bioengineering,
University of Utah,
Salt Lake City, UT 84112

Patrick J. McMahon
e-mail: mcmahonp@upmc.edu

Richard E. Debski
e-mail: genesis1@pitt.edu

Department of Bioengineering,
University of Pittsburgh,
Pittsburgh, PA 15219

The glenoid labrum is an integral component of the glenohumeral capsule's insertion into the glenoid, and changes in labrum geometry and mechanical properties may lead to the development of glenohumeral joint pathology. The objective of this research was to determine the effect that changes in labrum thickness and modulus have on strains in the labrum and glenohumeral capsule during a simulated physical examination for anterior instability. A labrum was incorporated into a validated, subject-specific finite element model of the glenohumeral joint, and experimental kinematics were applied simulating application of an anterior load at 0 deg, 30 deg, and 60 deg of external rotation and 60 deg of glenohumeral abduction. The radial thickness of the labrum was varied to simulate thinning tissue, and the tensile modulus of the labrum was varied to simulate degenerating tissue. At 60 deg of external rotation, a thinning labrum increased the average and peak strains in the labrum, particularly in the labrum regions of the axillary pouch (increased 10.5% average strain) and anterior band (increased 7.5% average strain). These results suggest a cause-and-effect relationship between age-related decreases in labrum thickness and increases in labrum pathology. A degenerating labrum also increased the average and peak strains in the labrum, particularly in the labrum regions of the axillary pouch (increased 15.5% strain) and anterior band (increased 10.4% strain). This supports the concept that age-related labrum pathology may result from tissue degeneration. This work suggests that a shift in capsule reparative techniques may be needed in order to include the labrum, especially as activity levels in the aging population continue to increase. In the future validated, finite element models of the glenohumeral joint can be used to explore the efficacy of new repair techniques for glenoid labrum pathology.
[DOI: 10.1115/1.4002622]

1 Introduction

The glenohumeral joint is the most dislocated major joint in the body, and greater than 80% of dislocations occur in the anterior direction [1–3]. The inferior glenohumeral ligament (IGHL), composed of the anterior band of the inferior glenohumeral ligament (AB-IGHL), axillary pouch (AP), and posterior band of the inferior glenohumeral ligament (PB-IGHL), is the primary stabilizer at joint positions associated with anterior dislocation [4–6] and is often injured following dislocation [7–10]. Injuries include permanent deformation of the capsule [11–13] and humeral avulsion [14–17]; however, detachment of the inferior glenohumeral ligament at its insertion into the glenoid, particularly in the anterior/inferior region, is frequent and has been a target of repair for restoration of anterior stability [7,10,18–20].

An integral component of the glenoid insertion of the inferior glenohumeral ligament is the glenoid labrum, a vascularized ring of fibrous tissue extending distally from the glenoid [20–26]. The labrum provides an increased depth and concavity to the glenoid fossa for resistance to humeral head translation [21,22]. Additionally, the labrum serves as a transition zone between the deformable capsule and the more rigid glenoid, and its fibrillar connections to both structures help to transfer load across the joint [21,22,25,26].

Labrum pathology has been shown to increase with age. Increases in labrum tears in older age groups have been reported [27] along with an age-dependent increase in failures at the labrum during mechanical testing [9]. The tensile force necessary to cause rupture in the capsule/labrum complex has also been shown to decrease with age [20]. In addition to increases in labrum pathology, labrum radial thickness decreases with age [5,28], and the mechanical properties of the labrum may decrease with age due to tissue degeneration [28]. While aging may involve multiple factors that contribute to tissue weakening, a direct link may exist between the changes in labrum geometry and mechanical properties and the occurrence of labrum pathology. Furthermore, changes in the stability provided by the labrum may cause abnormal transfer of load between the capsule and glenoid or abnormal joint translations, subjecting the capsule to an increased risk of pathology.

Finite element modeling provides a powerful tool for analyzing the multiaxial stability provided by the soft tissue structures of the glenohumeral joint in clinically relevant joint positions. The distribution of strain in soft tissues has been used previously as a measure of the stability provided by the capsule and insertion site tissues [4,11,29–33]. Distributions of strain in the labrum and capsule can also be evaluated to identify the areas of these structures with the highest risk for pathology. Therefore, the overall objective of this work was to use a validated, subject-specific finite element model of the glenohumeral joint to determine the effects of changes in labrum thickness and modulus on strains in the labrum and capsule in the inferior glenohumeral ligament during a simulated physical examination for anterior instability. These

---

analyses were performed using an existing model to identify specific clinical implications of changes in labrum geometry and mechanical properties to risks of labrum and capsule pathology.

2 Materials and Methods

2.1 Finite Element Model Construction and Validation. A combined experimental and computational approach was used to construct and validate the subject-specific finite element model. The methodology has been detailed previously [34–37] and only brief descriptions of the model's development and validation are provided. The finite element model was constructed based on the surface geometry and tissue properties obtained from a fresh-frozen shoulder (male, 45 years old, left, without pathology) and included the following experimental inputs: (1) surface geometry of the humerus, scapula, and capsule regions; (2) joint kinematics during a clinically relevant physical examination for anterior instability; and (3) mechanical properties of the capsule regions. The experimental distribution of strain in the capsule during the physical examination was also calculated for validation of the model.

All soft tissues were removed except for the glenohumeral capsule and the coracohumeral ligament. A 7×11 grid of black delrin strain markers (1.58 mm diameter) was adhered to the inferior glenohumeral ligament mid-substance using cyanoacrylate, forming a 6×10 array of quadrilateral surface elements for validation. The reference configuration of the capsule strain markers, or the three-dimensional positions of the markers at the joint's reference position where slack in the capsule has been removed via inflation with compressed air, was then determined using a motion tracking system (DMAS, Spicatek, HI) [30,34,35,37,38]. This methodology is similar to recording measurements for strain calculations during uniaxial testing of soft tissues after a preload has been applied to remove slack in the tissue. Upon recording the reference configuration a computed tomography (CT) scan (GE® Lightspeed, Milwaukee, WI) was obtained with the joint in its reference position for use in determining the surface geometries of the humerus, scapula, and capsule.

The shoulder was subsequently subjected to a physical examination used for diagnosis of anterior instability using a robotic/universal force-moment sensor testing system [35,39–42]. Loaded joint positions were obtained following application of a 25 N anterior load to the humerus at 60 deg of glenohumeral abduction in the scapular plane, and 0 deg, 30 deg, and 60 deg of external rotation [43,44]. The three-dimensional positions of the capsule strain markers were recorded at these joint positions and defined as the strained configuration of the capsule strain markers. Upon completion of the experimental procedure, the reference configuration and strained configurations of the capsule strain markers were then inputted into ABAQUS® (v 6.7-1, Dassault Systemes, Lowell, MA), and the experimental distribution of strain in the midsubstance of the IGHL was obtained by computing the Green–Lagrange maximum principal strains in the quadrilateral elements. The motions of the humerus with respect to the scapula from the reference position to the loaded positions were obtained via digitization of registration blocks fixed to the humerus and scapula in both positions and defined using coordinate system transformations [45].

A combined experimental and computational approach was used to determine the material coefficients for the glenohumeral capsule [4,46,47]. A bidirectional mechanical testing protocol was performed on tissue samples from each capsule region (AB-IGHL, axillary pouch, PB-IGHL, anterosuperior region, and posterior region). The experimental testing was then simulated computationally, and an inverse finite element optimization routine was used to determine the material coefficients to an isotropic hypoelastic constitutive model. These coefficients were then inputted to the model to define the material properties of each capsule region.
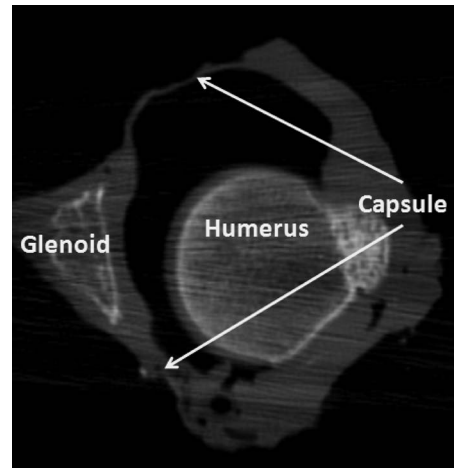

Fig. 1 Sample CT image of left shoulder with the joint in the reference position. The image depicts the difficulty in differentiating between the soft-tissue structures at the insertion of the capsule into the glenoid.

The surface geometries of the humerus, scapula, humeral head cartilage, and all capsule regions (AB-IGHL, axillary pouch, PB-IGHL, anterosuperior region, and posterior region) were manually segmented from the CT data set (SURFDRIVER v3.5.6) and the surfaces were imported into a finite element preprocessor (TRUEGRID, XYZ Scientific, Livermore, CA). Triangular surfaces representing the humerus and scapula were converted to rigid body shell meshes [48]. The humeral head cartilage was assigned rigid body brick elements, and each capsule region was meshed with quadrilateral YASE shell elements [49]. A 2.0 mm uniform thickness was assigned to the mesh of each capsule region based on experimental measurements of capsule thickness among different regions and published data [4,11]. Motion of the humerus with respect to the scapula was prescribed based on the coordinate system transformations obtained experimentally.

The nonlinear finite element solver NIKE3D was used for all analyses [31,36,47,50–52]. The positions of the capsule strain markers were incorporated into the model so that predicted strains could be computed in areas of the capsule that corresponded to the size and location of the quadrilateral elements. LSPOST (Livermore Software Technology Corporation, Livermore, CA) was then used to visualize and output predicted Green–Lagrange maximum principal strains in the quadrilateral elements. Validation of the model was performed by comparing experimental and predicted strains in the quadrilateral elements of the IGHL at the joint position with 60 deg of external rotation. In order for the predicted strains to be considered valid, the average difference between the experimental and predicted strain values had to be within two times the repeatability of the experimental methodology used to determine the strain distribution in the glenohumeral capsule or 7.0% strain [34,35]. The average difference between the experimental and predicted strains was 1.4%; therefore, the model was considered to be validated [34,35].

2.2 Inclusion and Modification of the Glenoid Labrum. Incorporation of the glenoid labrum into the validated, finite element model was constrained by experimental and computational limitations. The labrum was difficult to identify in the computed tomography images due to the fibrocartilagenous transition between capsule, labrum, and cartilage at the glenoid insertion site making identification of the separate structures challenging (Fig. 1). In addition, adding another structure to the glenoid rim would have changed the geometric surface boundaries of the capsule near its glenoid insertion, thus preventing one-to-one comparisons of capsule strains with the validated, finite element model. As a result, computational modification of the capsule shell elements at the
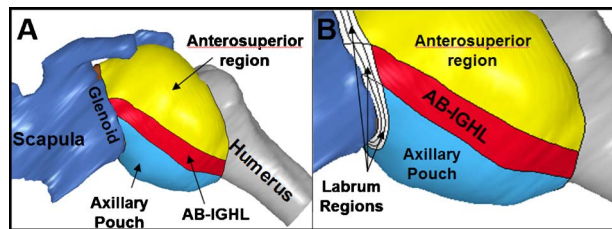
Fig. 2 (*A*) Anterior view of subject-specific finite element model (left shoulder). (*B*) Labrum regions added for current study.

glenoid insertion site was performed, with the labrum geometry and mechanical properties incorporated into the insertion site region without compromising the capsule.

The capsule elements inserting into the glenoid were redefined explicitly as labrum elements in the validated model, which served as the nominal model for the current analyses (Fig. 2). These elements were grouped into five labrum regions corresponding to the existing capsular regions and represented a direct capsule insertion into the labrum, a common capsule-labrum interface [26]. The labrum elements were defined so that the labrum depth (the dimension normal to the glenoid) was similar to the 2–4 mm labrum depth reported previously [21]. For the nominal model, the labrum was assigned shell elements and an isotropic constitutive model equivalent to the capsule, and no changes were made to the geometry (radial thickness was 2.0 mm) and mechanical properties (moduli of the AB-IGHL, axillary pouch, PB-IGHL, anterosuperior, and posterior regions were 2.05 MPa, 4.92 MPa, 3.73 MPa, 2.12 MPa, and 5.83 MPa, respectively) of these elements relative to the validated model. Therefore, the modulus of each labrum element was equivalent to the modulus of the neighboring capsule elements and thus not equivalent throughout the labrum circumference [53].

The thickness and modulus values for the labrum for the current study were obtained from the literature because the labrum geometry and properties could not be obtained experimentally. The radial thickness of the labrum throughout its circumference has been reported to be between 2.4 mm and 11.2 mm [22]; however, the inferior circumferential half of the labrum was found to have a radial thickness range between 2.4 mm and 4.5 mm. The labrum shape is also not constant throughout its periphery, and has been described as having radial cross sections of both triangular and rounded appearances [23,25]. Regardless of the shape, the radial thickness of the labrum decreases in the proximal-to-distal direction. Therefore, the labrum thickness modifications included a linear taper from a maximum radial thickness at the interface with the glenoid to a minimum radial thickness of 2.0 mm at the interface with the capsule, giving the labrum a wedge-shaped radial cross section. Two thickness models were created for analysis with the nominal model, containing a linear radial thickness taper of 4.0 mm (Thickness_4 model) and 6.0 mm (Thickness_6 model), respectively, at the interface with the glenoid to 2.0 mm at the interface with the capsule.

The tensile modulus of the labrum has been shown to vary throughout its circumference in animals [53]; thus, the labrum modulus was varied with respect to the corresponding capsule region modulus. The tensile modulus of the human labrum was reported to be 22.8 MPa [54], approximately five times higher than the tensile moduli of the capsule regions in the model. The compressive properties of the labrum have been reported as similar to those of the meniscus [22,55,56], a tissue with histological similarity to the labrum [23]. Based on the values described above and meniscal modulus data reported in the literature [57–59], two modulus modification models were created: a labrum modulus

two times (Modulus_2X model) or five times (Modulus_5X model) higher, respectively, than the modulus of the corresponding capsule region.

2.3 Data Analysis and Statistics. The nominal, Thickness_4, and Thickness_6 models were subjected to the kinematics of the three joint positions with 0 deg, 30 deg, and 60 deg of external rotation, to evaluate the effects of labrum thickness modification. Green–Lagrange maximum principal strains were calculated at the nodes in labrum region elements of the AB-IGHL, the axillary pouch, and the PB-IGHL. Average nodal strains were also calculated in the quadrilateral elements used for validation in the midsubstance of the AB-IGHL, as preliminary experimental data indicated that the AB-IGHL was repeatedly strained above the experimental strain repeatability of $\pm 3.5\%$ strain during the simulated physical examination [34]. The nodal strains were then averaged within each labrum region and among the capsule elements for analysis, in each model.

Friedman tests (SPSS, Apache Software, Chicago, IL) were used to determine statistically significant strain differences ($p < 0.05$) between a given labrum region or the capsule in the three thickness modification models, and Wilcoxon Signed Rank Tests with a Bonferroni correction were used for post hoc pairwise comparisons ($p < 0.017$). Significant pairwise differences were qualified with the requirements that they be statistically significant and greater than the experimental strain repeatability of $\pm 3.5\%$ strain.

The nominal, Modulus_2X, and Modulus_5X models were then used to analyze the effects from changes in labrum modulus. The methods performed with the labrum thickness analyses were repeated with the labrum modulus analyses, so that the effect of labrum modulus modification could also be determined in the labrum regions and capsule at the three joint positions.

Since high strains indicate areas of substantial load transfer and therefore risk for pathology, peak strains in the labrum regions and in the capsule region were also determined for each thickness and modulus model, at each of the three joint positions.

3 Results

3.1 Labrum Thickness Modifications. At the joint position with 60 deg of external rotation, strain in the labrum decreased as the labrum thickness taper was increased (Fig. 3). As the labrum thickness taper was increased from the nominal model to the Thickness_4 model to the Thickness_6 model, strain significantly decreased in the labrum regions of the AB-IGHL (23.6% to 16.1% to 12.3% strain) and axillary pouch (30.6% to 20.1% to 16.2% strain). Significant changes in strain occurred in all regions when comparing the nominal model to the Thickness_6 model, as strains decreased in the labrum region of the PB-IGHL (12.3–8.4% strain) and increased in the capsule (22.7–26.2% strain). The greatest changes in strain occurred in the labrum regions of the AB-IGHL and axillary pouch as the labrum thickness taper was increased from the nominal model to the Thickness_4 model, with decreases of 7.5% and 10.5% strains, respectively.

At the joint position with 30 deg of external rotation, as the labrum thickness taper was increased from the nominal model to the Thickness_4 model, strain significantly decreased in the labrum regions of the axillary pouch (27.9–19.3% strain) and PB-IGHL (15.8–12.1% strain). As the labrum thickness taper was further increased to that of the Thickness_6 model, strain significantly decreased only in the labrum region of the axillary pouch (19.3–15.2% strain). Significant changes in strain occurred in the axillary pouch and PB-IGHL (15.8–10.3% strain) when comparing the nominal model to the Thickness_6 model; however, the labrum thickness modifications did not significantly affect strains in the labrum region of the AB-IGHL or in the capsule. The greatest change in strain occurred in the labrum region of the axillary pouch as the labrum thickness taper was increased from the nominal model to the Thickness_4 model, a decrease of 10.6% strain.
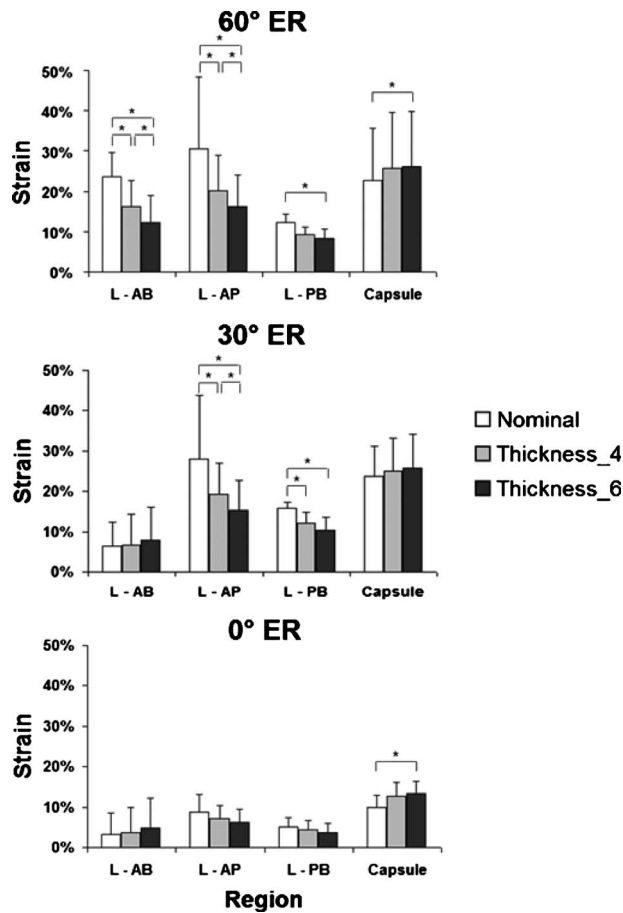
Fig. 3 The effect of modifying the labrum thickness at joint positions with a 25 N anterior load applied at 60 deg of glenohumeral abduction and 0 deg, 30 deg, and 60 deg of external rotation. L-AB, L-AP, and L-PB=labrum regions of the anterior band of the inferior glenohumeral ligament, axillary pouch, and posterior band of the inferior glenohumeral ligament, respectively (average±standard deviation of element strains within a labrum or capsule region). * statistical significance and difference greater than 3.5% strain.

At the joint position with 0 deg of external rotation, the labrum thickness taper modifications did not significantly affect the labrum regions of the AB-IGHL, axillary pouch, or PB-IGHL. Significant changes in strain occurred only in the capsule when comparing the nominal model to the Thickness_6 model (9.9–13.4% strain).

At the joint position with 60 deg of external rotation, peak strain in the labrum region of the axillary pouch decreased from 85% strain to 38% strain when the labrum thickness taper was increased from the nominal model to the Thickness_4 model (Table 1). Peak strains in the other labrum regions and the capsule were not greater than 48% strain in the nominal, Thickness_4, and Thickness_6 models, and never changed within a region by more than 6% strain between the models. At the joint position with 30 deg of external rotation, peak strain in the labrum region of the axillary pouch decreased from 84% strain to 31% strain when the labrum thickness taper was increased from the nominal model to the Thickness_4 model. Peak strains in the other labrum regions and the capsule were not greater than 39% strain in the nominal, Thickness_4, and Thickness_6 models, and never changed within a region by more than 11% strain between the models. At the joint position with 0 deg of external rotation, peak strains in all labrum regions and the capsule were not greater than 31% strain in the

Table 1 Peak strains in the labrum regions and capsule elements with the labrum thickness modifications at joint positions with a 25 N anterior load applied at 60 deg of glenohumeral abduction and 0 deg, 30 deg, and 60 deg of external rotation. L-AB, L-AP, L-PB=labrum regions of the anterior band of the inferior glenohumeral ligament, axillary pouch, and posterior band of the inferior glenohumeral ligament, respectively.

External rotation (deg)	Region	Thickness modification		
		Nominal (%)	Thickness_4 (%)	Thickness_6 (%)
60	L-AB	40	38	34
	L-AP	85	38	36
	L-PB	17	12	13
	Capsule	42	48	44
30	L-AB	28	35	39
	L-AP	84	31	32
	L-PB	18	18	18
	Capsule	33	38	38
0	L-AB	22	25	31
	L-AP	26	19	22
	L-PB	9	9	8
	Capsule	14	19	19

nominal, Thickness_4, and Thickness_6 models, and never changed within a region by more than 9% strain between the models.

3.2 Labrum Modulus Modifications. At the joint position with 60 deg of external rotation, strain in the labrum decreased as the labrum modulus was increased (Fig. 4). As the labrum modulus was increased from the nominal model to the Modulus_2X model, strain significantly decreased in the labrum regions of the AB-IGHL (23.6–13.3% strain), axillary pouch (30.6–15.1% strain), and the PB-IGHL (12.3–7.7% strain), and significantly increased in the capsule (22.7–26.5% strain). As the labrum modulus was further increased to that of the Modulus_5X model, strain significantly decreased in the labrum regions of the AB-IGHL (13.3–6.6% strain) and axillary pouch (15.1–8.2% strain). Significant changes in strain occurred in all regions when comparing the nominal model to the Modulus_5X model, as strain decreased in the PB-IGHL (12.3–4.4% strain) and increased in the capsule (22.7–28.0% strain). The greatest changes in strain occurred in the labrum regions of the AB-IGHL and axillary pouch as the modulus was increased from the nominal model to the Modulus_2X model, decreases of 10.4% and 15.5% strains, respectively.

At the joint position with 30 deg of external rotation, as the labrum modulus was increased from the nominal model to the Modulus_2X model to the Modulus_5X model, strain significantly decreased in the labrum regions of the axillary pouch (27.8% to 15.0% to 8.3% strain) and PB-IGHL (15.8% to 10.3% to 5.7% strain). Significant changes in strain occurred in the labrum regions of the axillary pouch and PB-IGHL as well as in the capsule (increased from 23.8% to 28.9% strain) when comparing the nominal model to the Modulus_5X model. However, the labrum modulus modifications did not significantly affect strains in the labrum region of the AB-IGHL. The greatest change in strain occurred in the labrum region of the axillary pouch as the modulus was increased from the nominal model to the Modulus_2X model, a decrease of 12.9% strain.

At the joint position with 0 deg of external rotation, the labrum modulus modifications did not significantly affect strains in the labrum regions of the AB-IGHL and PB-IGHL. Significant changes in strain occurred only in the labrum region of the axillary pouch (decreased from 8.7% to 3.7% strain) and the capsule
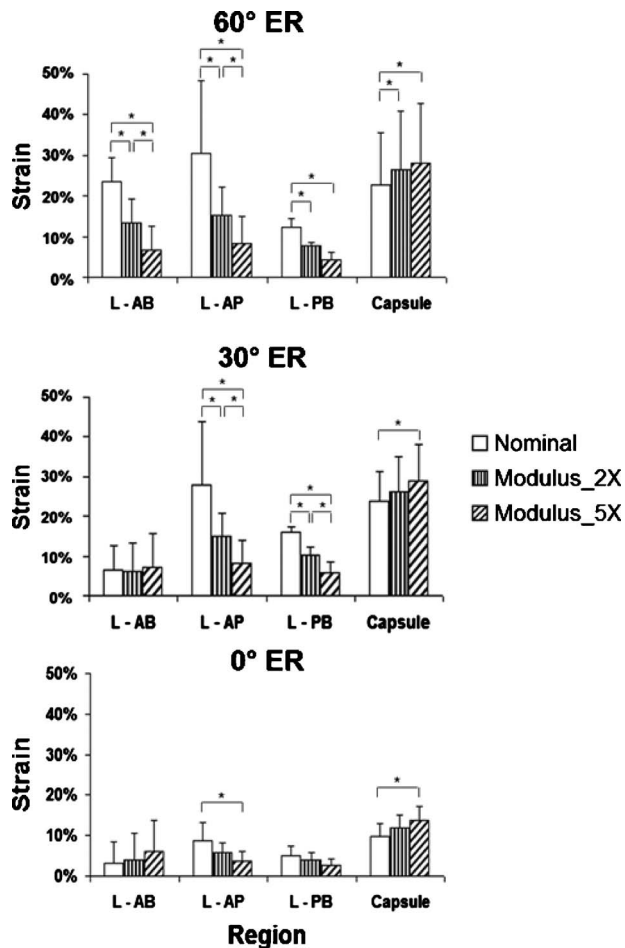
60° ER

30° ER

0° ER

Fig. 4 The effect of modifying the labrum modulus at joint positions with a 25 N anterior load applied at 60 deg of glenohumeral abduction and 0 deg, 30 deg, and 60 deg of external rotation. L-AB, L-AP, L-PB=labrum regions of the anterior band of the inferior glenohumeral ligament, axillary pouch, and posterior band of the inferior glenohumeral ligament, respectively (average±standard deviation of element strains within a labrum or capsule region). [*] statistical significance and difference greater than 3.5% strain.

Table 2 Peak strains in the labrum regions and capsule elements with the labrum modulus modifications at joint positions with a 25 N anterior load applied at 60 deg of glenohumeral abduction and 0 deg, 30 deg, and 60 deg of external rotation. L-AB, L-AP, L-PB=labrum regions of the anterior band of the inferior glenohumeral ligament, axillary pouch, and posterior band of the inferior glenohumeral ligament, respectively.

External rotation (deg)	Region	Modulus modification		
		Nominal (%)	Modulus_2X (%)	Modulus_5X (%)
60	L-AB	40	34	26
	L-AP	85	31	29
	L-PB	17	9	9
	Capsule	42	49	50
30	L-AB	28	34	37
	L-AP	84	26	26
	L-PB	18	15	13
	Capsule	33	41	44
0	L-AB	22	27	32
	L-AP	26	18	20
	L-PB	9	8	7
	Capsule	14	18	21

4 Discussion

In this study, the glenoid labrum was incorporated into a validated, subject-specific finite element model of the glenohumeral joint, and the labrum thickness and modulus were modified to examine the effects on strains in the labrum and capsule in clinically relevant joint positions. When an anterior load was applied to the abducted joint at external rotation angles beyond 30 deg, a decreasing labrum thickness caused strains in the labrum to increase, particularly in the labrum regions of the AB-IGHL and the axillary pouch. Lowering the labrum modulus to less than twice that of the neighboring capsule regions (i.e., in the nominal model) also caused strains in the labrum to reach higher magnitudes, particularly in the labrum regions of the AB-IGHL and the axillary pouch. When the labrum was removed peak strains in the labrum regions of the axillary pouch more than doubled when compared with models having a labrum. The peak strain in the capsule, however, remained relatively constant whether the labrum was present or not.

The data suggest that there may exist an increased risk of pathology to the labrum, particularly the labrum regions of the axillary pouch and the AB-IGHL, when the labrum thickness decreases. This conclusion indicates a potential correlation between the decreases in labrum thickness and increases in labrum pathology that occur with age. Furthermore, this work contributes to the understanding of Bankart lesion pathology to the anterior-inferior capsule-labrum region following anterior dislocation [19], as the anterior-inferior region of the labrum is the thinnest region of the labrum tissue [22].

Additionally, the results of the labrum modulus analyses suggest that a decreased labrum modulus may pose an increased risk for pathology to the labrum. A decreased labrum modulus may result from degeneration of the labrum tissue such as occurs with age, which may also help explain the clinically observed age-related increases in labrum pathology. This is in accordance with age-related degenerations of other fibrocartilagenous tissues, as increased pathology to the knee meniscus in older populations is believed to be from tissue degeneration [60].

The kinematics used in this study represents a physical examination for anterior instability, in which anterior loads are applied to the humerus when the joint is abducted and externally rotated. However, at joint positions where the capsule becomes the primary anterior stabilizer (i.e., 30 deg and 60 deg of external rota-

(increased from 9.9% to 13.8% strain) when comparing the nominal model to the Modulus_5X model.

At the joint position with 60 deg of external rotation, peak strain in the labrum region of the axillary pouch decreased from 85% strain to 31% strain when the labrum modulus was increased from the nominal model to the Modulus_2X model (Table 2). Peak strains in the other labrum regions and the capsule were not greater than 50% strain in the nominal, Modulus_2X, and Modulus_5X models, and never changed within a region by more than 14% strain between the models. At the joint position with 30 deg of external rotation, peak strain in the labrum region of the axillary pouch decreased from 84% strain to 26% strain when the labrum modulus was increased from the nominal model to the Modulus_2X model. Peak strains in the other labrum regions and the capsule were not greater than 44% strain in the nominal, Modulus_2X, and Modulus_5X models, and never changed within a region by more than 11% strain between the models. At the joint position with 0 deg of external rotation, peak strains in all labrum regions and the capsule were not greater than 32% strain in the nominal, Thickness_4, and Thickness_6 models, and never changed within a region by more than 10% strain between the models.

tion), the strains in the labrum with decreased thickness or modulus became highest. A thinning or degenerating labrum might therefore be subjected to a greater risk of pathology during dislocation, when loads transferred in the joint are much higher. Since the changes in labrum thickness or modulus had relatively little effect at the joint position with 0 deg of external rotation, a thinning or degenerating labrum may have a larger impact in those individuals who frequently position their joint near its end range of motion, such as throwing athletes or individuals with occupations requiring overhead motion. Typically these motions are frequent among younger, more active individuals; however, the increasing activity levels of the aging population may result in a considerable increase in labrum pathology among the population than is currently seen today.

The data from the current work have implications regarding clinical treatments of capsule-labrum pathology. The high average and peak strains in the insertion site of the nominal model suggest that without the increased thickness and modulus provided by the labrum at the insertion site, the risk for pathology in the insertion site will increase during subsequent patient activity. Current repair procedures for glenohumeral joint instability involve plicating loose capsule tissue and suturing it directly to the glenoid, creating a new capsule insertion site without a labrum. This scenario is represented by the nominal model in the current work, in which the risk for pathology to the capsule's insertion site was found to be greatest without a soft-tissue transition between the deformable capsule and rigid glenoid. The results of this study therefore suggest that a shift in reparative treatment procedures may be necessary to restore the full stability provided by the capsule's insertion site and avoid subsequent recurrence and reoperation. These treatment procedures will apply to the entire population regardless of patient demographic, as the absence of a soft-tissue transition between the capsule and glenoid have similar risks of pathology regardless of subject-specific variability in capsule/labrum geometry and mechanical properties.

The experimental and computational average and peak strains in the capsule recorded in the current study compare well with previous studies that computed multiaxial strain in the capsule in similar joint positions [30,34]. A limitation of the current work is that experimental strains in the labrum were not collected during the initial finite element model development due to experimental constraints. However, the average labrum strains in the anterior-inferior labrum regions reported in the current work compare well with previously collected labrum strain data. Rizio et al. [61] and Pradhan et al. [62] reported the average labrum strain in the posterior-superior labrum to be approximately 4–15% during throwing motions. While the labrum region and joint motions analyzed in the current study differ from the previous studies, the strain values in the current work (approximately 3–15%) closely match those reported previously. The high strains in the insertion site are consistent with previous work [11] that reported the average failure strain in isolated regions of the inferior glenohumeral ligament to be higher in bone-capsule-bone complexes (27% strain) than in the midsubstance (11% strain). The magnitude of the failure strains are lower than the values reported in this work; however, this may be attributed to the reporting of unidirectional strains in the referenced study versus multidirectional maximum principal strains in this study. Since collagen fibers in the capsule are randomly oriented [63] and the capsule is deformed in multiple directions during anterior loading [30,34,39], unidirectional strain measurements may underestimate the strain in the soft tissue structures.

The capsule insertion into the labrum in the current work was modeled as a direct insertion, while previous histological analysis has shown that the capsule can also partially insert into the neck of the glenoid [26]. However, all types of glenohumeral capsule insertions have connections between the labrum and capsule formed by intermingling of the fibers of the two tissues, which our model represents. In addition, only one shoulder was analyzed in

this study with labrum thickness and modulus values taken from the literature, and the effects of subject-specific age, gender, race, and surface geometry were not evaluated. However, the data in the current study provide valuable insight into the effects that labrum thickness and modulus variations have on strains in the labrum and capsule. In addition, the effects of a thinning or degenerating labrum on the risks for labrum and capsule pathology should be independent of moderate variations in subject-specific inputs. In the future, the computational approach utilized in this study can be used as a powerful tool for examining the ability of repair procedures to restore the function of the labrum and capsule following injury or degeneration.

Acknowledgment

References

[1] Hawkins, R. J., and Mohtadi, N. G., 1991, "Controversy in Anterior Shoulder Instability," Clin. Orthop. Relat. Res., (272), pp. 152–161.
[2] Cave, E., Burke, J., and Boyd, R., 1974, *Trauma Management*, Year Book Medical, Chicago, IL.
[3] Kirkley, A., Griffin, S., Richards, C., Miniaci, A., and Mohtadi, N., 1999, "Prospective Randomized Clinical Trial Comparing the Effectiveness of Immediate Arthroscopic Stabilization Versus Immobilization and Rehabilitation in First Traumatic Anterior Dislocations of the Shoulder," Arthroscopy, 15(5), pp. 507–514.
[4] Ellis, B. J., Debski, R. E., Moore, S. M., McMahon, P. J., and Weiss, J. A., 2007, "Methodology and Sensitivity Studies for Finite Element Modeling of the Inferior Glenohumeral Ligament Complex," J. Biomech., 40(3), pp. 603–612.
[5] Gohlke, F., Essigkrug, B., and Schmitz, F., 1994, "The Patterns of the Collagen Fiber Bundles of the Capsule of the Glenohumeral Joint," J. Shoulder Elbow Surg., 3(3), pp. 111–128.
[6] Turkel, S. J., Panio, M. W., Marshall, J. L., and Girgis, F. G., 1981, "Stabilizing Mechanisms Preventing Anterior Dislocation of the Glenohumeral Joint," J. Bone Jt. Surg., Am. Vol., 63(8), pp. 1208–1217.
[7] Caspari, R. B., 1988, "Arthroscopic Reconstruction for Anterior Shoulder Instability," Oper. Tech. Orthop., 3, pp. 59–66.
[8] Field, L. D., Bokor, D. J., and Savoie, F. H., III, 1997, "Humeral and Glenoid Detachment of the Anterior Inferior Glenohumeral Ligament: A Cause of Anterior Shoulder Instability," J. Shoulder Elbow Surg., 6(1), pp. 6–10.
[9] Lee, T. Q., Dettling, J., Sandusky, M. D., and McMahon, P. J., 1999, "Age Related Biomechanical Properties of the Glenoid-Anterior Band of the Inferior Glenohumeral Ligament-Humerus Complex," Clin. Biomech. (Bristol, Avon), 14(7), pp. 471–476.
[10] Morgan, C. D., and Bodenstab, A. B., 1987, "Arthroscopic Bankart Suture Repair: Technique and Early Results," Arthroscopy, 3(2), pp. 111–122.
[11] Bigliani, L. U., Pollock, R. G., Soslowsky, L. J., Flatow, E. L., Pawluk, R. J., and Mow, V. C., 1992, "Tensile Properties of the Inferior Glenohumeral Ligament," J. Orthop. Res., 10(2), pp. 187–197.
[12] Schneider, D. J., Tibone, J. E., McGarry, M. H., Grossman, M. G., Veneziani, S., and Lee, T. Q., 2005, "Biomechanical Evaluation after Five and Ten Millimeter Anterior Glenohumeral Capsulorrhaphy Using a Novel Shoulder Model of Increased Laxity," J. Shoulder Elbow Surg., 14(3), pp. 318–323.
[13] Remia, L. F., Ravalin, R. V., Lemly, K. S., McGarry, M. H., Kvitne, R. S., and Lee, T. Q., 2003, "Biomechanical Evaluation of Multidirectional Glenohumeral Instability and Repair," Clin. Orthop. Relat. Res., (416), pp. 225–236.
[14] Bokor, D. J., Conboy, V. B., and Olson, C., 1999, "Anterior Instability of the Glenohumeral Joint With Humeral Avulsion of the Glenohumeral Ligament. A Review of 41 Cases," J. Bone Jt. Surg., Br. Vol., 81(1), pp. 93–96.
[15] Bui-Mansfield, L. T., Taylor, D. C., Uhorchak, J. M., and Tenuta, J. J., 2002, "Humeral Avulsions of the Glenohumeral Ligament: Imaging Features and a Review of the Literature," AJR, Am. J. Roentgenol., 179(3), pp. 649–655.
[16] Chhabra, A., Diduch, D. R., and Anderson, M., 2004, "Arthroscopic Repair of a Posterior Humeral Avulsion of the Inferior Glenohumeral Ligament (HAGL) Lesion," Arthroscopy, 20, pp. 73–76.
[17] Warner, J. J., and Beim, G. M., 1997, "Combined Bankart and HAGL Lesion Associated With Anterior Shoulder Instability," Arthroscopy, 13(6), pp. 749–752.
[18] Seeger, L. L., Gold, R. H., and Bassett, L. W., 1988, "Shoulder Instability: Evaluation With MR Imaging," Radiology, 168(3), pp. 695–697.
[19] Bankart, A. S., 1923, "Recurrent or Habitual Dislocation of the Shoulder-Joint," BMJ, 2, pp. 1132–1133.
[20] Hara, H., Ito, N., and Iwasaki, K., 1996, "Strength of the Glenoid Labrum and Adjacent Shoulder Capsule," J. Shoulder Elbow Surg., 5(4), pp. 263–268.
[21] Howell, S. M., and Galinat, B. J., 1989, "The Glenoid-Labral Socket. A Constrained Articular Surface," Clin. Orthop. Relat. Res., (243), pp. 122–125.
[22] Carey, J., Small, C. F., and Pichora, D. R., 2000, "In Situ Compressive Properties of the Glenoid Labrum," J. Biomed. Mater. Res., 51(4), pp. 711–716.
[23] Cooper, D. E., Arnoczky, S. P., O'Brien, S. J., Warren, R. F., DiCarlo, E., and Allen, A. A., 1992, "Anatomy, Histology, and Vascularity of the Glenoid La-

brum. An Anatomical Study," J. Bone Joint Surg. Am., **74**(1), pp. 46–52.

[24] Rao, A. G., Kim, T. K., Chronopoulos, E., and McFarland, E. G., 2003, "Anatomical Vriants in the Aterosuperior Apect of the Genoid Lbrum: A Statistical Analysis of Seventy-Three Cases," J. Bone Jt. Surg., Am. Vol., **85-A**(4), pp. 653–659.

[25] Nishida, K., Hashizume, H., Toda, K., and Inoue, H., 1996, "Histologic and Scanning Electron Microscopic Study of the Glenoid Labrum," J. Shoulder Elbow Surg., **5**(2), pp. 132–138.

[26] Eberly, V. C., McMahon, P. J., and Lee, T. Q., 2002, "Variation in the Glenoid Origin of the Anteroinferior Glenohumeral Capsulolabrum," Clin. Orthop. Relat. Res., (400), pp. 26–31.

[27] Pfahler, M., Haraida, S., Schulz, C., Anetzberger, H., Refior, H. J., Bauer, G. S., and Bigliani, L. U., 2003, "Age-Related Changes of the Glenoid Labrum in Normal Shoulders," J. Shoulder Elbow Surg., **12**(1), pp. 40–52.

[28] Prodromos, C. C., Ferry, J. A., Schiller, A. L., and Zarins, B., 1990, "Histological Studies of the Glenoid Labrum From Fetal Life to Old Age," J. Bone Jt. Surg., Am. Vol., **72**(9), pp. 1344–1348.

[29] McMahon, P. J., Dettling, J., Sandusky, M. D., Tibone, J. E., and Lee, T. Q., 1999, "The Anterior Band of the Inferior Glenohumeral Ligament. Assessment of Its Permanent Deformation and the Anatomy of Its Glenoid Attachment," J. Bone Jt. Surg., Br. Vol., **81**(3), pp. 406–413.

[30] Malicky, D. M., Soslowsky, L. J., Kuhn, J. E., Bey, M. J., Mouro, C. M., Raz, J. A., and Liu, C. A., 2001, "Total Strain Fields of the Antero-Inferior Shoulder Capsule Under Subluxation: A Stereoradiogrammetric Study," ASME J. Biomech. Eng., **123**(5), pp. 425–431.

[31] Debski, R. E., Weiss, J. A., Newman, W. J., Moore, S. M., and McMahon, P. J., 2005, "Stress and Strain in the Anterior Band of The Inferior Glenohumeral Ligament During a Simulated Clinical Examination," J. Shoulder Elbow Surg., **14**(1), pp. S24–S31.

[32] Kawada, T., Abe, T., Yamamoto, K., Hirokawa, S., Soejima, T., Tanaka, N., and Inoue, A., 1999, "Analysis Of Strain Distribution in the Medial Collateral Ligament Using a Photoelastic Coating Method," Med. Eng. Phys., **21**(5), pp. 279–291.

[33] Spalazzi, J. P., Gallina, J., Fung-Kee-Fung, S. D., Konofagou, E. E., and Lu, H. H., 2006, "Elastographic Imaging of Strain Distribution in the Anterior Cruciate Ligament and at the Ligament-Bone Insertions," J. Orthop. Res., **24**(10), pp. 2001–2010.

[34] Moore, S. M., Stehle, J. H., Rainis, E. J., McMahon, P. J., and Debski, R. E., 2008, "The Current Anatomical Description of the Inferior Glenohumeral Ligament Does Not Correlate With Its Functional Role in Positions of External Rotation," J. Orthop. Res., **26**(12), pp. 1598–1604.

[35] Moore, S. M., Ellis, B., Weiss, J. A., McMahon, P. J., and Debski, R. E., 2010, "The Glenohumeral Capsule Should Be Evaluated as a Sheet of Fibrous Tissue: A Validated Finite Element Model," Ann. Biomed. Eng., **38**(1), pp. 66–76.

[36] Ellis, B., Drury, N. J., Moore, S. M., McMahon, P. J., Weiss, J. A., and Debski, R. E., 2009, "Finite Element Modelling of the Glenohumeral Capsule Can Help Assess the Tested Region During a Clinical Exam," Comput. Methods Biomech. Biomed. Eng., **13**(3), pp. 413–418.

[37] Drury, N. J., 2008, *Evaluating the Anterior Stability Provided by the Glenohumeral Capsule: A Finite Element Approach*, University of Pittsburgh, Pittsburgh, PA.

[38] Malicky, D. M., Kuhn, J. E., Frisancho, J. C., Lindholm, S. R., Raz, J. A., and Soslowsky, L. J., 2002, "Neer Award 2001: Nonrecoverable Strain Fields of the Anteroinferior Glenohumeral Capsule Under Subluxation," J. Shoulder Elbow Surg., **11**(6), pp. 529–540.

[39] Debski, R. E., Wong, E. K., Woo, S. L.-Y., Sakane, M., Fu, F. H., and Warner, J. J., 1999, "In Situ Force Distribution in the Glenohumeral Joint Capsule During Anterior-Posterior Loading," J. Orthop. Res., **17**(5), pp. 769–776.

[40] Burkart, A. C., and Debski, R. E., 2002, "Anatomy and Function of the Glenohumeral Ligaments in Anterior Shoulder Instability," Clin. Orthop. Relat. Res., (400), pp. 32–39.

[41] Fujie, H., Livesay, G. A., Woo, S. L., Kashiwaguchi, S., and Blomstrom, G., 1995, "The Use of a Universal Force-Moment Sensor to Determine In-Situ Forces in Ligaments: a New Methodology," ASME J. Biomech. Eng., **117**(1), pp. 1–7.

[42] Woo, S. L., Debski, R. E., Wong, E. K., Yagi, M., and Tarinelli, D., 1999, "Use of Robotic Technology for Diathrodial Joint Research," J. Sci. Med. Sport, **2**(4), pp. 283–297.

[43] Moore, S. M., Musahl, V., McMahon, P. J., and Debski, R. E., 2004, "Multidirectional Kinematics of the Glenohumeral Joint During Simulated Simple Translation Tests: Impact on Clinical Diagnoses," J. Orthop. Res., **22**(4), pp. 889–894.

[44] Musahl, V., Moore, S. M., McMahon, P. J., and Debski, R. E., 2006, "Orientation Feedback During Simulated Simple Translation Tests Has Little Clinical Significance on the Magnitude and Precision of Glenohumeral Joint Translations," Knee Surg. Sports Traumatol. Arthrosc., **14**(11), pp. 1194–1199.

[45] Fischer, K. J., Manson, T. T., Pfaeffle, H. J., Tomaino, M. M., and Woo, S. L., 2001, "A Method for Measuring Joint Kinematics Designed for Accurate Registration of Kinematic Data to Models Constructed From CT Data," J. Biomech., **34**(3), pp. 377–383.

[46] Weiss, J. A., Gardiner, J. C., and Bonifasi-Lista, C., 2002, "Ligament Material Behavior Is Nonlinear, Viscoelastic and Rate-Independent Under Shear Loading," J. Biomech., **35**(7), pp. 943–950.

[47] Weiss, K. S., and Savoie, F. H., III, 2002, "Recent Advances in Arthroscopic Repair of Traumatic Anterior Glenohumeral Instability," Clin. Orthop. Relat. Res., (400), pp. 117–122.

[48] Maker, B. N., 1995, "Rigid Bodies for Metal Forming Analysis With NIKE3D," in University of California, Lawrence Livermore Laboratory, Technical Report No. UCRL-JC-119862.

[49] Engelmann, B. E., Whirley, R. G., and Goudreau, G. L., 1989, "A Simple Shell Element Formulation for Large-Scale Elastoplastic Analysis," *Analytical and Computational Models of Shells*, The American Society of Mechanical Engineers, New York, CED-Vol 3.

[50] Ellis, B. J., Lujan, T. J., Dalton, M. S., and Weiss, J. A., 2006, "Medial Collateral Ligament Insertion Site and Contact Forces in the ACL-Deficient Knee," J. Orthop. Res., **24**(4), pp. 800–810.

[51] Weiss, J. A., Maker, B. N., and Govindjee, S., 1996, "Finite Element Implementation of Incompressible, Transversely Isotropic Hyperelasticity," Comput. Methods Appl. Mech. Eng., **135**, pp. 107–128.

[52] Weiss, J. A., Schauer, D. A., and Gardiner, J. C., 1996, "Modeling Contact in Biological Joints Using Penalty and Augmented Lagrangian Methods," ASME Winter Annual Meeting, pp. 347–348.

[53] Ferguson, S. J., Bryant, J. T., and Ito, K., 2001, "The Material Properties of the Bovine Acetabular Labrum," J. Orthop. Res., **19**(5), pp. 887–896.

[54] Smith, C. D., Masouros, S. D., Hill, A. M., Wallace, A. L., Amis, A. A., and Bull, A. M., 2008, "Tensile Properties of the Human Glenoid Labrum," J. Anat., **212**(1), pp. 49–54.

[55] Joshi, M. D., Suh, J. K., Marui, T., and Woo, S. L., 1995, "Interspecies Variation of Compressive Biomechanical Properties of the Meniscus," J. Biomed. Mater. Res., **29**(7), pp. 823–828.

[56] Smith, C. D., Masouros, S. D., Hill, A. M., Wallace, A. L., Amis, A. A., and Bull, A. M., 2009, "The Compressive Behavior of the Human Glenoid Labrum May Explain the Common Patterns of SLAP Lesions," Arthroscopy, **25**(5), pp. 504–509.

[57] Lechner, K., Hull, M. L., and Howell, S. M., 2000, "Is the Circumferential Tensile Modulus Within a Human Medial Meniscus Affected by the Test Sample Location and Cross-Sectional Area?," J. Orthop. Res., **18**(6), pp. 945–951.

[58] Fithian, D. C., Kelly, M. A., and Mow, V. C., 1990, "Material Properties and structure-function relationships in the Menisci," Clin. Orthop. Relat. Res., (252), pp. 19–31.

[59] Tissakht, M., and Ahmed, A. M., 1995, "Tensile Stress-Strain Characteristics of the Human Meniscal Material," J. Biomech., **28**(4), pp. 411–422.

[60] 2002, *Orthopaedic Sports Medicine*, J. DeLee and D. Drez, eds., Elsevier Science, Philadelphia, PA.

[61] Rizio, L., Garcia, J., Renard, R., and Got, C., 2007, "Anterior Instability Increases Superior Labral Strain in the Late Cocking Phase of Throwing," Orthopedics, **30**(7), pp. 544–550.

[62] Pradhan, R. L., Itoi, E., Hatakeyama, Y., Urayama, M., and Sato, K., 2001, "Superior Labral Strain During The Throwing Motion. A Cadaveric Study," Am. J. Sports Med., **29**(4), pp. 488–492.

[63] Debski, R. E., Moore, S. M., Mercer, J. L., Sacks, M. S., and McMahon, P. J., 2003, "The Collagen Fibers of the Anteroinferior Capsulolabrum Have Multiaxial Orientation to Resist Shoulder Dislocation," J. Shoulder Elbow Surg., **12**(3), pp. 247–252.